sensors

Article

Thermally Stable Wireless Patch Antenna Sensor for Strain and Crack Sensing

Dan Li [1], **Yang Wang** [1,2,*]

[1] School of Civil and Environmental Engineering, Georgia Institute of Technology, Atlanta, GA
[2] School of Electrical and Computer Engineering, Georgia Institute of Technology, Atlanta, GA
* Correspondence: yang.wang@ce.gatech.edu

Received: date; Accepted: date; Published: date

Abstract: Strain and crack are critical indicators of structural safety. As a novel sensing device, a patch antenna sensor can be utilized to wirelessly estimate structural strain and surface crack growth through resonance frequency shift. Main challenges for the sensor are other effects such as temperature fluctuation that can generate unwanted resonance frequency shift and result in large noise in the measurement. Another challenge for existing designs of patch antenna sensor is the limited interrogation distance. In this research, thermally stable patch antenna sensors are investigated for more reliable measurement. Fabricated on a substrate material with steady dielectric constant, a new passive (battery-free) patch antenna sensor is designed to improve reliability under temperature fluctuations. In addition, another newly designed dual-mode patch antenna sensor is proposed to achieve a longer interrogation distance. Extensive experiments are conducted to characterize the patch antenna sensor performance, including thermal stability, tensile strain sensing, and emulated crack sensing. The two new patch antenna sensors are demonstrated to be effective in wireless strain and crack measurements and have potential applications in structural health monitoring (SHM).

Keywords: patch antenna sensor; RFID; thermal stability; energy harvesting; strain; crack; wireless sensing

1. Introduction

Civil structures, such as buildings and bridges, can suffer from damage caused by various types of loads during the life span. Without proper maintenance, the damage can adversely affect the performance of a structure and may even result in structural failure. Structural health monitoring (SHM) systems can advance time-based maintenance into more effective condition-based maintenance by periodically measuring structural responses. Among the measurements, strain is often an important indicator for stress concentration and crack development. Traditional strain measurements usually rely on metal foil strain gages and fiber optical sensors. However, these sensing technologies require lengthy cables for data acquisition and power supply, which increase the overall installation and maintenance cost of the whole monitoring system and limit the deployment scale.

The development of wireless communication technology has facilitated more convenient application of SHM systems on large structures. A typical wireless sensing system consists of a server and multiple sensor nodes. The server coordinates the wireless sensing network and receives measurement data from all the sensor nodes. Each sensor node usually has at least an embedded processor and a wireless transceiver. The advantageous features of onboard computing and wireless communication enable the dense and rapid deployment of sensor nodes. During past decades, various wireless sensing systems have been developed for SHM. For example, a low-cost wireless modular monitoring system was first proposed by Straser and Kiremidjian [1]. Among others, Lynch, *et al.* [2] and Wang, *et al.* [3] developed wireless sensing platforms that are validated on numerous civil structures. Kane, *et al.* [4] later proposed an extensible dual-core wireless sensing node, named Martlet, which provides more powerful onboard processing [5-8]. The Mote series (Imote and Imote2) wireless sensing systems have also been deployed for full-scale monitoring of civil infrastructures [9-11]. Extensive literature reviews about wireless sensing systems related to SHM applications can be found in [12,13]. Nevertheless, although the wireless sensing systems have achieved success in field deployment, the requirement of onboard battery power remains a difficulty for long-term application [14]. Many sensor locations on a large structure may not have reliable source for energy harvesting.

Even with reliable solar power, rechargeable batteries may need frequent replacement when operating in the outdoor environment.

To address the challenge of power source, passive (battery-free) wireless sensors have been proposed and studied. With integration of technologies such as near field communication (NFC) and radiofrequency identification (RFID), passive wireless sensors harvest energy from the interrogation signal and do not require onboard power supply. Among various passive wireless sensors for strain measurement, antenna sensors stand out for its simple configuration and low cost [14]. The sensing mechanism relies on the fact that the electromagnetic resonance frequency of an antenna depends on its dimension [15]. Based on this physics principle, the wirelessly identified resonance frequency shift of an antenna sensor can be utilized to estimate the strain applied on it. Due to the lack of onboard power, various signal modulation methods for passive antenna sensors have been investigated to increase the reliability of wireless communication. Deshmukh and Huang [16] proposed to use light-activated microwave impedance switch to change the phase of the antenna backscattering signal, which can be distinguished from environmental reflections. Frequency doubling technique using a Schottky diode is another signal modulation method for passive antenna sensors [17]. In addition, the RFID technology provides a convenient way to modulate the response signal of passive antenna sensors [18,19]. Finally, more literature review on passive antenna sensor for strain measurement can be found in survey articles [20,21].

Although extensive simulations and experiments have validated the strain and crack sensing performance of passive antenna sensors, thermal stability and limited interrogation range still remain as major challenges for reliable measurement. Besides structural strain, other environmental disturbances, such as temperature fluctuation, can also result in the resonance frequency shift of the antenna by changing the dielectric constant of antenna substrate. A large frequency shift due to temperature fluctuation brings difficulty in distinguishing strain and crack effects from the temperature effect. In order to improve the strain and crack sensing performance during temperature fluctuation, this research proposes RFID antenna sensors with a thermally stable substrate material.

Another limitation of the passive antenna sensor is the relatively short interrogation distance, due to lack of onboard power source. To increase the interrogation distance, we study the design of a dual-mode patch antenna sensor, which can automatically switch between passive and active modes. Toward the dual mode operation, the patch antenna sensor is attached with a power management circuitry. Incorporated with a solar cell, the circuitry can charge a coin cell battery and actively power the RFID chip when sunlight is available. In this active mode, the sensor requires less radiofrequency (RF) power for responding to reader interrogation, and thus achieves longer interrogation distance. On the other hand, when the battery power is depleted, or the battery dies from long-time outdoor operation, the sensor can still operate in passive mode, solely relying on the RF power from the reader interrogation. In summary, the dual-mode patch antenna sensor maintains the reliability of passive wireless sensors while providing the advantage of the long interrogation distance of active wireless sensors.

The rest of the paper is organized as follows. Section 2 describes the designs of two thermally stable patch antenna sensors, including the passive patch antenna sensor and the dual-mode patch antenna sensor. Section 3 introduces the strain and crack sensing mechanism of the patch antenna sensors, and the wireless sensing system for the RFID based antenna sensors. Section 4 presents the outdoor temperature experiment for validating the thermal stability of the passive antenna sensor. Section 5 describes the tensile test results for evaluating the strain sensing performance of the dual-mode sensor in both the passive and active modes. Section 6 shows the experimental results illustrating the crack sensing performance of the passive antenna sensor. Section 7 provides a summary and future work.

2. Patch Antenna Sensor Designs

Among several types of antennas that can be used as strain and crack sensor, patch antenna and its variations are simple and low-profile. Previous research work has proposed the patch antenna sensor with RT/duroid® 5880 (manufactured by Rogers Corporation) substrate [18]. Although the sensor has shown good performance for wireless strain and crack sensing, research has proven that under temperature fluctuation, the design with RT/duroid® 5880 substrate undergoes large resonance frequency change, due to its large dielectric constant variation (approximately 125 ppm/°C) [22]. To improve sensor reliability to temperature fluctuation, a thermally stable substrate material RT/duroid® 6202 (manufactured by Rogers Corporation) is chosen as the new antenna substrate material. As the substrate provides more stable dielectric constant under temperature fluctuation, the patch antenna sensor is expected to have more consistent resonance frequency when temperature fluctuates. In addition, integrated with energy harvesting technology, a dual-mode patch antenna sensor is designed to achieve longer interrogation distance. Section 2.1 presents the design of the passive patch antenna sensor for strain and crack sensing. Section 2.2 shows the design of the dual-mode patch antenna sensor.

2.1. Passive Patch Antenna Sensor

This section describes the passive patch antenna sensor design. The sensor adopts RT/duroid® 6202 as substrate material which has more stable dielectric constant under temperature fluctuation. The material RT/duroid® 6202 is a poly-tetra-fluoro-ethylene (PTFE) composite with limited woven glass reinforcement. The low dielectric constant ($\beta_{\mathrm{r}} = 2.90$) offers suitable electrical property for antenna sensor design. The low thermal coefficient of dielectric constant (5 ppm/°C) improves the sensor reliability when ambient temperature fluctuates. The thickness of the substrate is 30 milli-inches which balances the interrogation range and strain transfer ratio, *i.e.* the ratio of the strain on top copper cladding of the antenna over the strain on base structure.

The SL3S1013 RFID chip (manufactured by NXP Semiconductors) is chosen for wireless communication. The RFID chip contains a 96-bit tag identifier including 48-bit factory locked unique serial number. Equipped with advanced anti-collision mechanism, the RFID chip enables the reader to simultaneously access multiple antenna sensors nearby. The small footprint (0.0394×0.0571 inches^2) of the RFID chip further reduces the total size of the antenna sensor. The broad operation frequency range (from 840 MHz to 960 MHz) of the RFID chip facilitates international usage. The chip's high sensitivity and low power design provide long interrogation range of the passive patch antenna sensor. In addition, the compatibility with external power enables the design of dual-mode patch antenna sensor, which achieves longer interrogation range and is described in Section 2.2.

Figure 1 shows the front view of the passive patch antenna sensor. The total size of the antenna sensor is 2.17×2.36 inches². The sensor adopts a quarter-wave rectangular patch (folded-patch) antenna topology [23]. The top copper and the ground plane are connected through vias, allowing about 50% reduction to the footprint size of the patch antenna. The length of the top copper cladding is designed so that resonance frequency of the antenna sensor achieves about 900 MHz RFID band. To enable efficient power transfer, the length of matching lines is tuned to achieve impedance matching between the RFID chip (21.2−*j*199.7 Ω in passive mode) and the patch antenna.

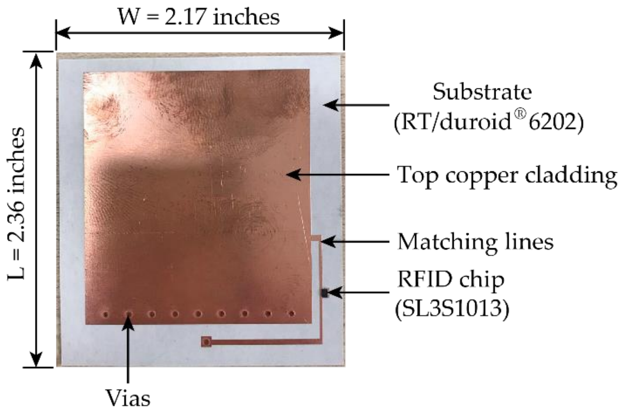

Figure 1 Prototype of passive patch antenna sensor

2.2. Dual-Mode Patch Antenna Sensor

This section describes the dual-mode patch antenna sensor design. Despite the advantages of operating without onboard power supply, the passive patch antenna sensor can only support limited interrogation range. In order to increase the interrogation distance, a dual-mode RFID antenna sensor is designed. Figure 2 shows the design drawing and picture of the prototype dual-mode patch antenna sensor. The total size of the antenna sensor is 2.44×4.69 inches². Both the drawing and picture show that a patch antenna sensor and a power management circuitry are fabricated on the same piece of substrate. Equipped with the power management circuitry, this sensor is capable of harvesting solar energy, storing energy in a rechargeable coin battery, and operating in active mode. When the battery runs out, this dual-mode RFID patch antenna sensor can automatically fall back to passive mode.

The patch antenna sensor is designed in a similar way as described in Section 2.1. The matching lines are redesigned for efficient power transfer between the RFID chip and the patch antenna. In active mode, the RFID chip operates with impedance of 6.9−*j*205.5 Ω. The designed matching lines have to balance the impedance matching between passive mode and active mode, and ensure the patch antenna to operate reliably at about 900 MHz for both modes.

The power management circuitry derives energy from solar radiation and supplies regulated voltage to the RFID chip. The energy harvesting IC (integrated circuit) chip MAX17710 (manufactured by Maxim Integrated) is adopted for this application. This IC chip both charges a cell battery with over-charge protection and powers the RFID chip with over-discharge protection. The harvested solar energy is stored in a high-capacity Lithium-Ion rechargeable coin cell battery RJD2032C1T1 (manufactured by Illinois Capacitor), which improves the reliability of the patch antenna sensor.

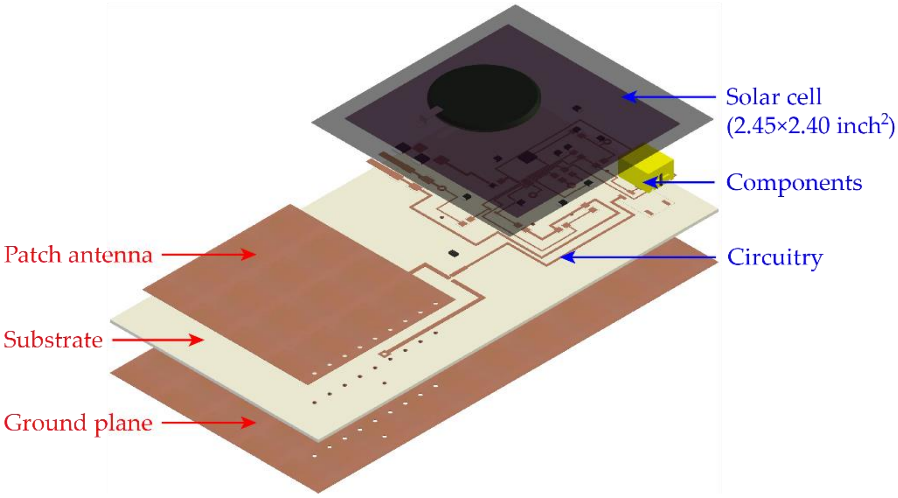

(a) Design drawing

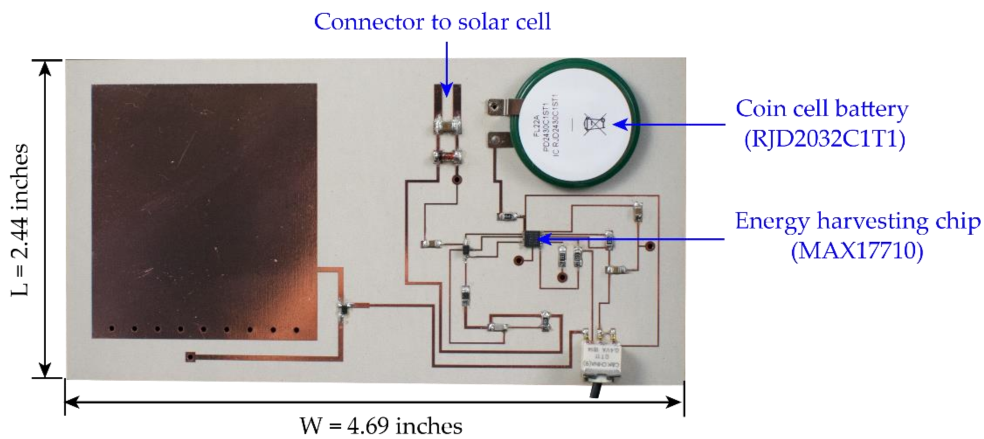

(b) Picture of dual-mode patch antenna sensor (solar cell removed)

Figure 2 Dual-mode patch antenna sensor

3. Wireless Sensing and Measurement Mechanism

The strain/crack induced resonance frequency shift of the antenna sensor can be wireless detected and utilized to estimate the structural strain and surface crack propagation. Section 3.1 introduces the sensing mechanism of the patch antenna sensor. Section 3.2 describes the wireless measurement mechanism of the RFID based patch antenna sensing system.

3.1. Sensing Mechanism

This section describes the sensing mechanism of patch antenna sensors. A patch antenna sensor can wirelessly measure strain and/or crack on a structural surface through the shift of its electromagnetic resonance frequency. Figure 3 illustrates the patch antenna sensor design. The RFID chip is mounted on the top side of the dielectric substrate and used for wireless communication. The matching lines are designed to achieve the best impedance matching between the RFID chip and the antenna.

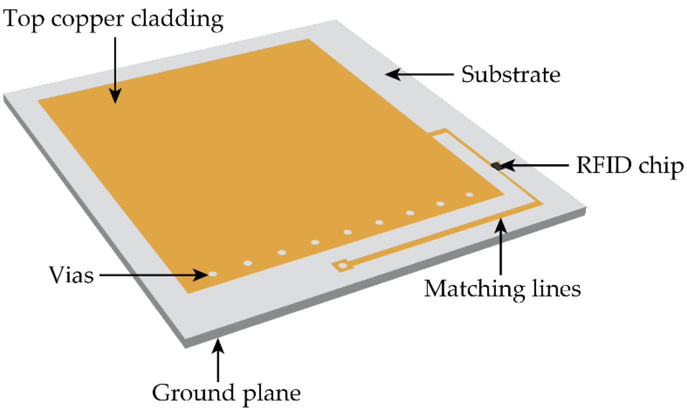

Figure 3 Illustration of the patch antenna sensor

According to electromagnetic theory, the resonance frequency f_R of a folded patch antenna at certain temperature T can be calculated as:

$$f_R(0,T) = \frac{c}{4L\sqrt{\beta_r(T)}} \tag{1}$$

where c is the speed of light; L is the length of the patch antenna; β_r is the effective dielectric constant of the substrate depending on temperature T.

When strain ε is applied, the length of the patch antenna changes from L to $L(1+\varepsilon)$. In SHM application on civil structures, the dimensionless ε is usually on the order of 10^{-5} (10 micro-strains) to 10^{-3} (1,000 micro-strains). If the effective dielectric constant of the substrate remains as constant, the change of resonance frequency Δf of the patch antenna due to strain ε can be calculated as:

$$\Delta f(T) = f_{\mathrm{R}}(\varepsilon, T) - f_{\mathrm{R}}(0,T) = \frac{f_{\mathrm{R}}(0,T)}{1+\varepsilon} - f_{\mathrm{R}}(0,T) \approx -f_{\mathrm{R}}(0,T)\varepsilon = S(T)\varepsilon \tag{2}$$

Here $S(T)$ is the theoretical strain sensitivity of the folded patch antenna sensor at temperature T. As shown in Eq. (2), at a constant ambient temperature, the change of resonance frequency Δf of the patch antenna has an approximately linear relationship with strain ε, especially when the strain ε is small. This approximately linear relationship indicates that by wirelessly measuring the antenna resonance frequency, the applied strain can be derived.

3.2. Wireless Measurement Mechanism

This section describes the wireless measurement mechanism of the RFID based patch antenna sensor. To wirelessly obtain the resonance frequency, an RFID reader Tagformance Lite (manufactured by Voyantic Ltd.) is used to interrogate the patch antenna sensor. Figure 4 shows the overview of the wireless sensing system composed of an RFID reader and a dual-mode patch antenna sensor. Upon measurement, the reader emits an RF interrogation signal to the sensor at a specific frequency. The patch antenna sensor captures the signal and transmits the energy to the RFID chip. When the captured power reaches the activation threshold, the RFID chip modulates and sends the reflection signal to the reader. After receiving the reflection signal, the reader records the transmitted power and repeats the same procedure at the next frequency point. The interrogation power curve (Figure 4(b)) can be obtained once the reader sweeps through the interested frequency band. When the sensor operates in passive mode, the RF signal from the reader is the only power source for exciting the RFID chip, and thus the sensor needs relatively high interrogation power for wireless communication (blue curves in Figure 4(b)). When in active mode with onboard battery power, excitation of the RFID chip requires less interrogation power (red curves in Figure 4(b)). The resonance frequency of the patch antenna sensor refers to the frequency at which minimum amount of interrogation power is required to excite the RFID chip. When the antenna sensor deforms together with based structure, the resonance frequency shifts according to the structural strain.

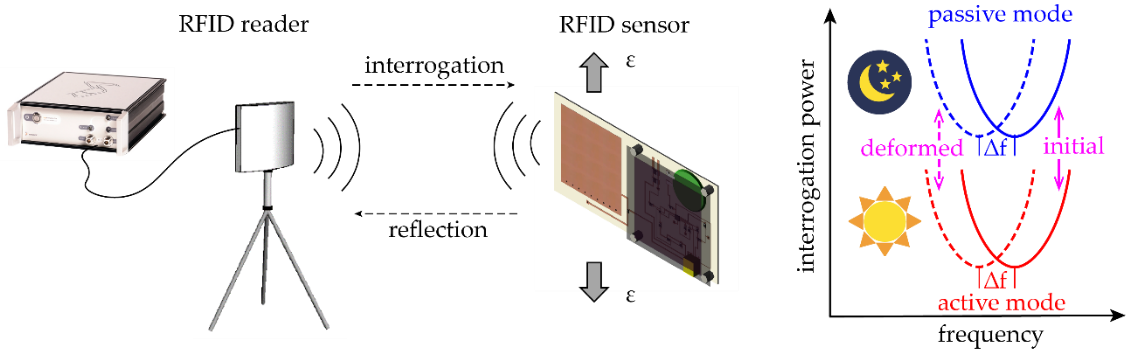

(a) Wireless sensing system (b) Interrogation power curve

Figure 4 Illustration of wireless sensing system for the patch antenna sensor

4. Thermal Stability Test

An outdoor temperature test is conducted to study the influence of the temperature fluctuation on the resonance frequency of the antenna sensors. Figure 5 shows the outdoor experiment setup. Two antenna sensors, one with RT/duroid® 5880 substrate and the other with RT/duroid® 6202 substrate, are installed on the web surface of a steel I-section column. Metal foil strain gages are installed to measure the temperature induced strain on the steel column surface. To keep track of temperature fluctuations in the field, two thermocouples are installed near the sensors. A reader antenna is placed 12 inches away from patch antenna sensors for wireless interrogation.

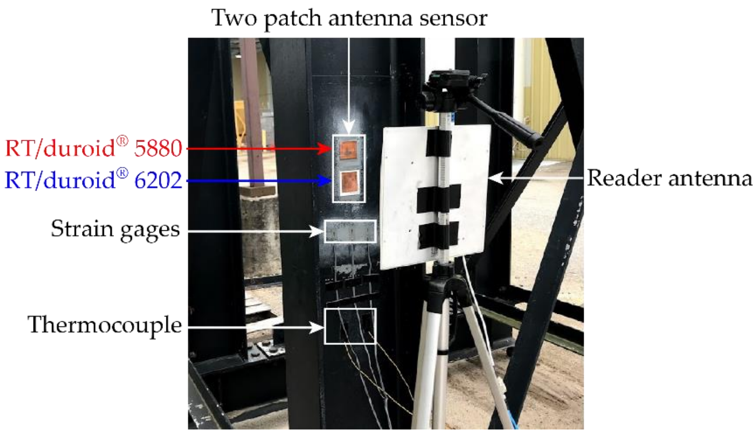

Figure 5 Experimental setup for outdoor temperature test

The outdoor test starts at noon with ambient temperature at around 76 ˚F. The temperature is measured every 20 minutes until 17:00. The temperature fluctuation is plotted in Figure 6. The highest temperature is around 80 ˚F and the lowest temperature is around 70 ˚F. At each time step, interrogation power threshold is measured for both patch antenna sensors. To reduce measurement noise, the reader antenna sweeps through the target frequency span five times for each measurement. Then the average among the five interrogation power threshold curves is calculated. Resonance frequencies of both patch antenna sensors are extracted from the average interrogation power threshold curves and shown in Figure 6. A total of ~ 0.5 MHz resonance frequency change is observed on patch antenna sensor with RT/duroid® 5880 substrate during the test. Meanwhile, the patch antenna senor with RT/duroid® 6202 substrate shows a total of ~ 0.1 MHz resonance frequency change, which is much less than that of the previous design with RT/duroid® 5880 substrate.

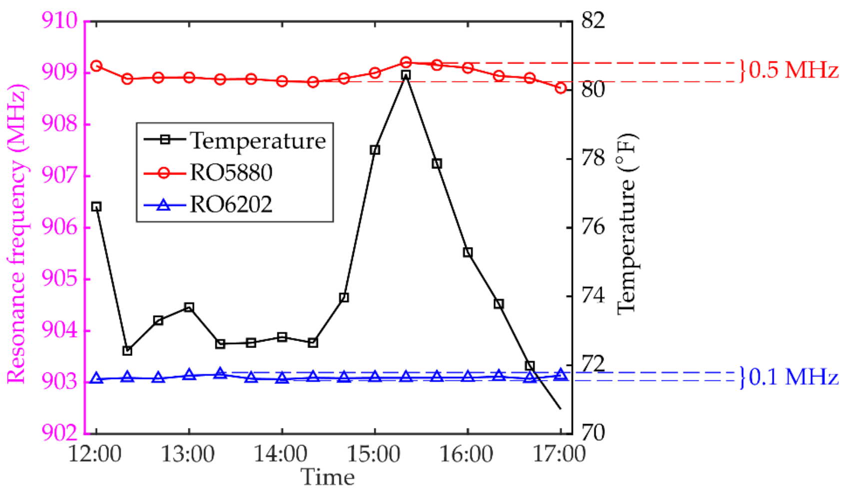

Figure 6 Resonance frequency change due to temperature fluctuation

5. Strain Sensing Test

Laboratory tensile tests are conducted to evaluate the strain sensing performance of the dual-mode patch antenna sensor. Figure 7 shows the experimental setup for tensile test on the dual-mode patch antenna sensor. The patch antenna sensor and reference metal foil strain gages are installed in the middle of an aluminum specimen. An 18 dBi high-gain Yagi antenna is used as the interrogation reader antenna. The interrogation distance between the patch antenna sensor and the reader antenna is set as 36 inches for passive mode test and 60 inches for active mode test.

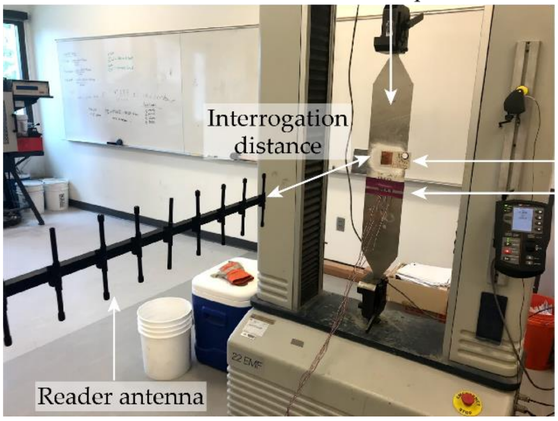

Figure 7 Experimental setup for tensile test

5.1. Passive Mode Test

This section describes tensile strain sensing performance of the dual-mode patch antenna sensor working in passive mode. The load applied by the tensile machine is configured so that approximately each loading step generates a 50 με strain increment. From 0 to about 300 με, a total of seven loading steps are tested. The interrogation power threshold of the patch antenna sensor is measured at each loading step. For each measurement, again five frequency sweeps are conducted for averaging. The average interrogation power threshold curves at different loading steps/strain levels are plotted in Figure 8(a). For clarity, the figure only plots the interrogation power curves of four strain levels. The test results show that the interrogation power for passive mode is from 22 dBm to 27 dBm.

Resonance frequency of the patch antenna sensor at each strain level is determined by peak picking of each average interrogation power threshold curve. As expected, the resonance frequency decreases as the tensile strain increases. Figure 8(b) plots the resonance frequency change with the strain. Linear regression is applied on these data points, and the strain sensitivity is calculated as −599 Hz/με. In addition, the coefficient of determination is 0.9871, confirming the approximately linear relationship between resonance frequency and strain.

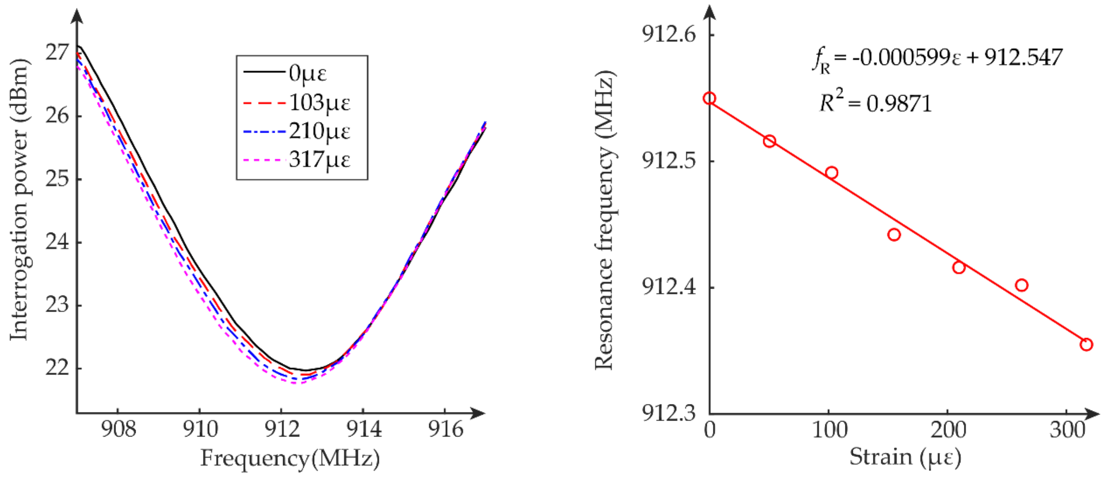

(a) Average interrogation power threshold (b) Resonance frequency f_R versus strain ε

Figure 8 Tensile test results of passive mode test

5.2. Active Mode Test

This section describes tensile strain sensing performance of the dual-mode patch antenna sensor working in active mode. The interrogation distance is increased to 60 inches, about 1.67 times longer than that of the passive mode test. All the other experimental setup and data analysis method are the same as before. The average interrogation power threshold curves at different loading steps/strain levels are plotted in Figure 9(a). For clarity, the figure only plots the interrogation power curves of four strain levels. The test results show that the interrogation power for active mode is from 22 dBm to 26 dBm, which is similar to the power level for passive mode as shown in Section 5.1. This confirms that using similar amount of interrogation power, the patch antenna sensor achieves longer interrogation distance at active mode.

Resonance frequency of the patch antenna sensor at each strain level is determined by peak picking of each average interrogation power threshold curve. As expected, the resonance frequency decreases as the tensile strain increases. Figure 9(b) plots the resonance frequency change with the strain. Linear regression is applied on these data points, and the strain sensitivity is calculated as −582 Hz/με. In addition, the coefficient of determination is 0.9787, confirming the approximately linear relationship between resonance frequency and strain.

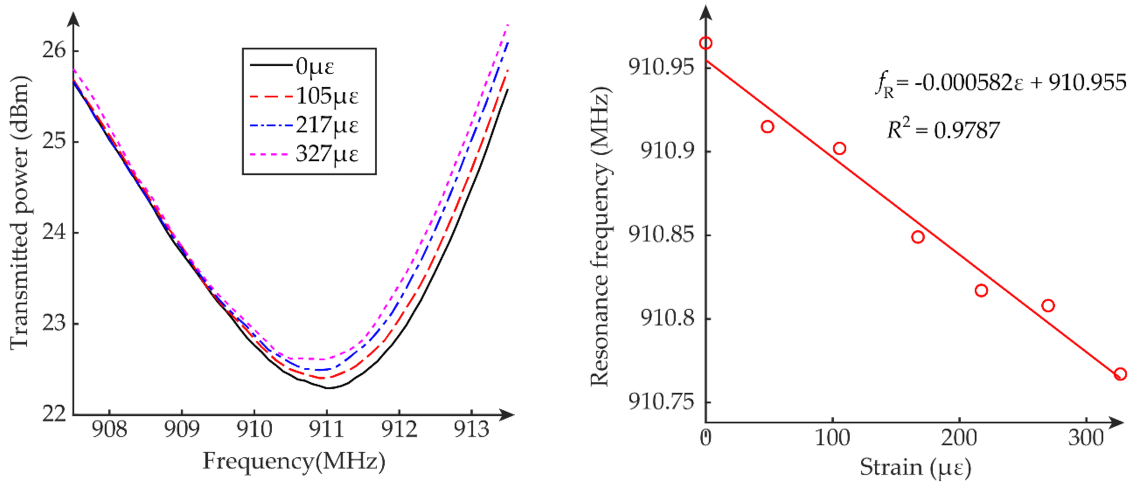

(a) Average interrogation power threshold (b) Resonance frequency f_R versus strain ε

Figure 9 Tensile test results of active mode test

6. Crack Sensing Test

To investigate crack sensing performance of the patch antenna sensor, an emulated crack test is conducted. To conveniently emulate crack propagation, a special crack testing device (Figure 10) is designed for the experiments. The crack testing device consists of three aluminum plates, i.e. a base plate, a rotating top plate, and a fixed bottom plate. Due to their thickness, all three plates can be assumed to remain rigid during crack testing for the sensor. The fixed bottom plate is fastened to the base plate by four corner bolts. The rotating top plate is attached to the base plate by one bolt at the bottom right corner, which acts as the rotation axis. A fine-resolution displacement control screw is installed at the top left corner of the rotating plate. By turning the screw, a rotation is imposed on the top plate and a crack/gap is opened between the top and bottom plates. The crack opening size is measured by a digital dial gage (0.0001 in. resolution) mounted at the left side of the base plate. A spring-loaded probe from the gage pushes against an angle bracket that is fastened to the left edge of the rotating plate.

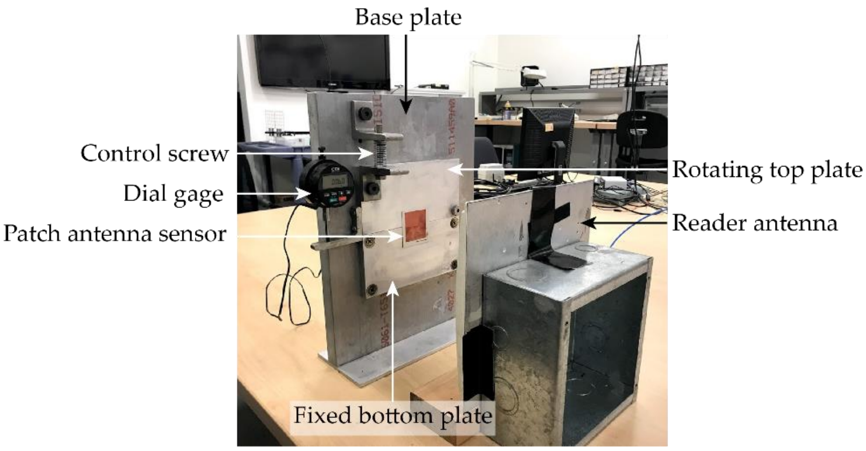

Figure 10 Experimental setup for emulated crack test

For crack sensing, the antenna sensor is bonded on the rotating and fixed plates, above the gap and at the center of the crack opening line, as shown in Figure 10. The panel reader antenna faces the center of the patch antenna sensor at a distance of 12 inches. At each gap opening size, the Tagformance reader sweeps through a frequency band and measures the interrogation power threshold, so that the resonance frequency of the antenna sensor can be determined. After the reader finishes interrogation at one gap opening size, the displacement control screw is turned to reach the next gap opening size and the measurement is repeated.

In total, eleven gap opening sizes are wirelessly measured during the experiment. The resonance frequencies extracted from interrogation power curves are plotted in Figure 11. For clarity, only four representative photos of the deformed/cracked antenna sensor are shown in the plot. No fracture but slight deformation occurs on the sensor when the gap opening size is smaller than 10 milli-inches. When the gap opening size is larger than 20 milli-inches, the crack starts to propagate on the top surface of the sensor. After the gap opening size reaches 40 milli-inches, the crack grows through the entire antenna width and no response from the antenna sensor can be received by the Tagformance reader.

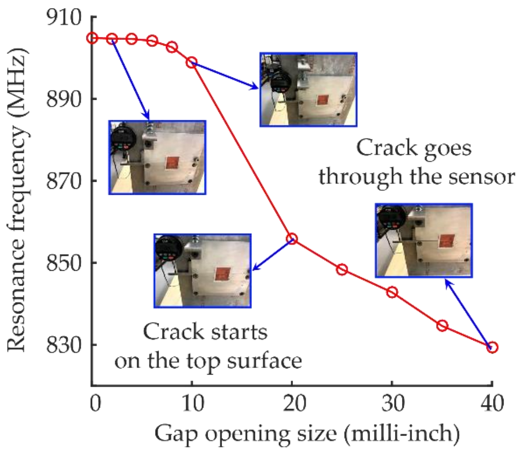

Figure 11 Resonance frequency f_R versus gap opening size at dial gage

7. Summary and Future Work

In this paper, thermally stable patch antenna sensors have been designed and validated for monitoring strain and crack growth of civil structures. Extensive experiments lead to following conclusions. The temperature induced dielectric constant change can result in unwanted resonance frequency change in patch antenna sensors. The thermally stable substrate material is capable of improving the strain and crack sensing performance of patch antenna sensors by preserving the dielectric constant at different temperature levels. The tensile test results demonstrate that the developed patch antenna sensors are capable of measuring small structural strain by wireless identifying the resonance frequency shift. In addition, working in active mode, the dual-mode patch antenna sensor can achieve longer interrogation distance with the assistance of solar charged battery power. The emulated crack sensing test results show that the designed patch antenna sensor is capable of tracking surface crack propagation. As the crack grows, the resonance frequency of the patch antenna sensor decreases as expected.

Future research can investigate calibration according to temperature effects to further eliminate the unwanted uncertainties in the strain and crack measurements. Sensor performance may also be fine-tuned through more detailed multiphysics modelling and simulation.

Author Contributions: Conceptualization, D.L. and Y.W.; methodology, D.L. and Y.W.; software, D.L. and Y.W.; validation, D.L. and Y.W.; formal analysis, D.L. and Y.W.; investigation, D.L. and Y.W.; resources, Y.W.; data curation, D.L.; writing—original draft preparation, D.L. and Y.W.; writing—review and editing, D.L. and Y.W.;

visualization, D.L. and Y.W.; supervision, Y.W.; project administration, Y.W.; funding acquisition, Y.W. All authors have read and agreed to the published version of the manuscript.

Funding: This research is funded by provided by the U.S. Department of Transportation, Office of the Assistant Secretary for Research and Technology (USDOT/OST-R) under Grant No. 69A3551747126 through INSPIRE University Transportation Center (http://inspire-utc.mst.edu) at Missouri University of Science and Technology.

Acknowledgments: The authors would like to thank the anonymous reviewers for their valuable and insightful comments.

Conflict of Interests: The authors declare no conflict of interests. The funders had no role in the design of the study; in the collection, analyses, or interpretation of data; in the writing of the manuscript, or in the decision to publish the results.

REFERENCES

1. Straser, E.G.; Kiremidjian, A.S. *A Modular, Wireless Damage Monitoring System for Structures*; Report No. 128; John A. Blume Earthquake Engineering Center, Stanford University: Stanford, CA, 1998.
2. Lynch, J.P.; Law, K.H.; Kiremidjian, A.S.; Kenny, T.W.; Carryer, E.; Partridge, A. The design of a wireless sensing unit for structural health monitoring. In Proceedings of the 3rd International Workshop on Structural Health Monitoring, Stanford, CA, September 12-14, 2001.
3. Wang, Y.; Lynch, J.P.; Law, K.H. Validation of an integrated network system for real-time wireless monitoring of civil structures. In Proceedings of the 5th International Workshop on Structural Health Monitoring, Stanford, CA, September 12-14, 2005.
4. Kane, M.; Zhu, D.; Hirose, M.; Dong, X.; Winter, B.; Häckell, M.; Lynch, J.P.; Wang, Y.; Swartz, A. Development of an extensible dual-core wireless sensing node for cyber-physical systems. In Proceedings of SPIE, Sensors and Smart Structures Technologies for Civil, Mechanical, and Aerospace Systems, San Diego, CA, March 10-14, 2014.
5. Dong, X.; Chen, S.; Zhu, D.; Kane, M.; Wang, Y.; Lynch, J.P. High-speed heterogeneous data acquisition using Martlet - a next-generation wireless sensing device. In Proceedings of the 6th World Conference on Structural Control and Monitoring (6WCSCM), Barcelona, Spain, July 15-17, 2014.
6. Dong, X.; Liu, X.; Wright, T.; Wang, Y.; DesRoches, R. Validation of wireless sensing technology densely instrumented on a full-scale concrete frame structure. In Proceedings of International Conference on Smart Infrastructure and Construction (ICSIC), Cambridge. United Kingdom, June 27-29, 2016.
7. Dong, X.; Zhu, D.; Wang, Y.; Lynch, J.P.; Swartz, R.A. Design and validation of acceleration measurement using the Martlet wireless sensing system. In Proceedings of the ASME 2014 Conference on Smart Materials, Adaptive Structures and Intelligent Systems (SMASIS), Newport, RI, September 8-10, 2014.
8. Liu, X.; Dong, X.; Wang, Y. Field testing of Martlet wireless sensing system on an in-service pre-stressed concrete highway bridge. In Proceedings of SPIE, Health Monitoring of Structural and Biological Systems, Las Vegas, NV, March 20-24, 2016.
9. Zhao, F.; Guibas, L.J.; Guibas, L. *Wireless Sensor Networks: An Information Processing Approach*; Morgan Kaufmann: 2004.
10. Spencer, B.F.; Jo, H.; Mechitov, K.A.; Li, J.; Sim, S.-H.; Kim, R.E.; Cho, S.; Linderman, L.E.; Moinzadeh, P.; Giles, R.K. Recent advances in wireless smart sensors for multi-scale monitoring and control of civil infrastructure. *Journal of Civil Structural Health Monitoring* 2016, *6*, 17-41.
11. Nagayama, T.; Spencer, B.F.; Rice, J.A. Autonomous decentralized structural health monitoring using smart sensors. *Structural Control and Health Monitoring* 2009, *16*, 842-859.

12. Lynch, J.P.; Loh, K.J. A summary review of wireless sensors and sensor networks for structural health monitoring. *The Shock and Vibration Digest* 2006, *38*, 91-128.
13. Noel, A.B.; Abdaoui, A.; Elfouly, T.; Ahmed, M.H.; Badawy, A.; Shehata, M.S. Structural health monitoring using wireless sensor networks: A comprehensive survey. *IEEE Communications Surveys and Tutorials* 2017, *19*, 1403-1423.
14. Huang, H.; Chen, Z. Antenna sensors in passive wireless sensing systems. In *Handbook of Antenna Technologies*, Springer: Singapore, 2015; pp. 1-34.
15. Tata, U.; Huang, H.; Carter, R.L.; Chiao, J.C. Exploiting a patch antenna for strain measurements. *Measurement Science and Technology* 2009, *20*, 015201.
16. Deshmukh, S.; Huang, H. Wireless interrogation of passive antenna sensors. *Measurement Science and Technology* 2010, *21*, 035201.
17. Cho, C.; Yi, X.; Li, D.; Wang, Y.; Tentzeris, M.M. Passive wireless frequency doubling antenna sensor for strain and crack sensing. *IEEE Sensors J* 2016, *16*, 5725-5733.
18. Yi, X.; Wu, T.; Wang, Y.; Leon, R.T.; Tentzeris, M.M.; Lantz, G. Passive wireless smart-skin sensor using RFID-based folded patch antennas. *International Journal of Smart and Nano Materials* 2011, *2*, 22-38.
19. Yi, X.; Cho, C.; Wang, Y.; Tentzeris, M.M. Battery-free slotted patch antenna sensor for wireless strain and crack monitoring. *Smart Structures and Systems* 2016, *18*, 1217-1231.
20. Zhang, J.; Tian, G.Y.; Marindra, A.M.; Sunny, A.I.; Zhao, A.B. A review of passive RFID tag antenna-based sensors and systems for structural health monitoring applications. *Sensors* 2017, *17*, 265.
21. Deivasigamani, A.; Daliri, A.; Wang, C.; John, S. A review of passive wireless sensors for structural health monitoring. *Modern Applied Science* 2013, *7*, 57-76.
22. Yi, X.; Vyas, R.; Cho, C.; Fang, C.-H.; Cooper, J.; Wang, Y.; Leon, R.T.; Tentzeris, M.M. Thermal effects on a passive wireless antenna sensor for strain and crack sensing. In Proceedings of SPIE, Sensors and Smart Structures Technologies for Civil, Mechanical and Aerospace Systems, San Diego, CA, March 11-15, 2012.
23. Finkenzeller, K. *RFID Handbook*, 2nd ed.; John Wiley & Sons: New York, 2003.